Supplemental Information

Modulation of Transport Properties *via* S/Br Substitution: Solvothermal Synthesis, Crystal Structure, and Transport Properties of $Bi_{13}S_{17}Br_3$

Dinesh K. Amarasinghe,[a] Philip Yox,[a,b] Gayatri Viswanathan,[a,b] Adedoyin N. Adeyemi,[a] and Kirill Kovnir [a,b,*]

[a] *Department of Chemistry, Iowa State University, Ames, Iowa 50011, USA*

[b] *Ames National Laboratory, U.S. Department of Energy, Ames, Iowa 50011, USA*

*Corresponding Author. Email: kovnir@iastate.edu

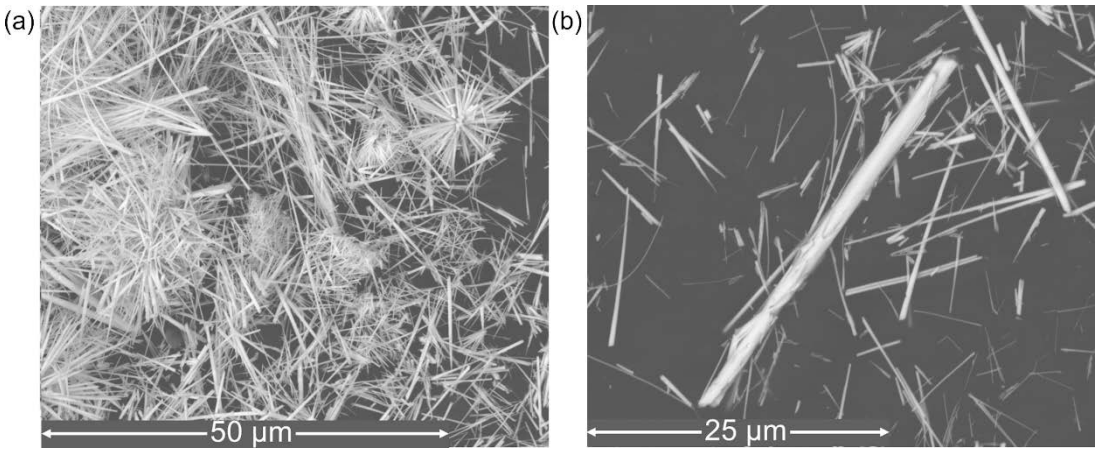

Fig. S1. Backscattered electron images of (a) $Bi_{13}S_{17}Br_3$ and (b) $Bi_{13}S_{18}I_2$ samples.

Table S1. Comparison of the elemental compositions from EDS analyses with the corresponding theoretical values for $Bi_{12.9}S_{17.2}Br_{2.9}$ and $Bi_{13}S_{18}I_2$.

Element	Atomic percentage (%)			
	$Bi_{12.9}S_{17.2}Br_{2.9}$		$Bi_{13}S_{18}I_2$	
	Theoretical	Experimental	Theoretical	Experimental
Bi	39.1	39.2(4)	39.4	39.5(2)
S	52.1	52.4(5)	54.5	53.7(2)
Br	8.8	8.4(4)		
I			6.1	6.8(2)

Table S2. Fractional atomic coordinates and isotropic displacement parameters of $Bi_{13}S_{17}Br_3$ obtained from SCXRD refinement.

	x/a	***y/b***	***z/c***	U_{iso} **(Å^2)**	**Occupancy**
Bi1	0.60958(7)	0.48268(6)	0.885(3)	0.0078(3)	1
Bi2a	0.70295(11)	0.75519(19)	0.378(3)	0.0054(4)	0.877(8)
Bi2b	0.7121(7)	0.7878(13)	0.359(7)	0.0054(4)	0.123
Bi3	0	0	0.012(6)	0.011(2)	0.21(2)
Bi4	0	0	0.726(5)	0.011(2)	0.24(2)
Br1	2/3	1/3	0.372(6)	0.005(1)	1
S1	0.8331(4)	0.8142(4)	0.882(6)	0.003(1)	1
S2	0.7383(3)	0.6006(3)	0.384(6)	0.010(1)	0.877(8)
Br2	0.7383(3)	0.6006(3)	0.384(6)	0.010(1)	0.123
S3	0.5477(4)	0.6105(4)	0.872(7)	0.001(2)	0.98(1)
Br3	0.5477(4)	0.6105(4)	0.872(7)	0.001(2)	0.02

Table S3. Selected interatomic distances for Bi1, Bi2a, Bi2b, Bi3, and Bi4 metal sites in the structure of $Bi_{13}S_{17}Br_3$ obtained from SCXRD refinement.

		Distance (Å)
Bi1–S2/Br2	× 1	2.765(17)
Bi1–S2/Br2	× 1	2.774(17)
Bi1–S3/Br3	× 1	2.593(5)
Bi1–S3/Br3	× 1	2.953(18)
Bi1–S3/Br3	× 1	2.879(18)
Bi2a–S1	× 1	2.667(17)
Bi2a–S1	× 1	3.027(5)
Bi2a–S1	× 1	2.646(18)
Bi2a–S2/Br2	× 1	2.708(5)
Bi2a–S3/Br3	× 1	3.085(17)
Bi2a–S3/Br3	× 1	3.050(17)
Bi2b–S1	× 1	2.56(3)
Bi2b–S1	× 1	2.593(18)
Bi2b–S1	× 1	2.70(3)
Bi2b–S2/Br2	× 1	3.121(18)
Bi2b–S2/Br2	× 1	3.15(2)
Bi2b–S2/Br2	× 1	3.27(2)
Bi3–S1	× 3	2.789(10)
Bi3–S1	× 3	3.12(2)
Bi4–S1	× 3	2.810(10)

Table S4. Selected angles for Bi1, Bi2a, Bi2b, Bi3, and Bi4 metal sites in the structure of $Bi_{13}S_{17}Br_3$ obtained from SCXRD refinement.

		Bond Angle (°)
S3/Br3–Bi1–S2/Br2	× 1	84.3(4)
S3/Br3–Bi1–S2/Br2	× 1	86.0(4)
S2/Br2–Bi1–S2/Br2	× 1	92.58(14)
S3/Br3–Bi1–S3/Br3	× 1	80.2(4)
S3/Br3–Bi1–S3/Br3	× 1	81.6(3)
S3/Br3–Bi1–S3/Br3	× 1	86.70(14)
S2/Br2–Bi1–S3/Br3	× 1	87.9(5)
S2/Br2–Bi1–S3/Br3	× 1	89.5(5)
S2/Br2–Bi1–S3/Br3	× 1	166.09(17)
S2/Br2–Bi1–S3/Br3	× 1	165.6(2)
S1–Bi2a–S1	× 1	97.80(17)
S1–Bi2a–S1	× 1	73.1(3)
S1–Bi2a–S1	× 1	72.9(3)
S1–Bi2a–S2/Br2	× 1	81.7(4)
S1–Bi2a–S2/Br2	× 1	81.1(4)
S1–Bi2a–S2/Br2	× 1	140.41(14)
S1–Bi2a–S3/Br3	× 1	86.8(5)
S1–Bi2a–S3/Br3	× 1	86.5(5)
S1–Bi2a–S3/Br3	× 1	157.5(3)
S1–Bi2a–S3/Br3	× 1	157.8(3)
S1–Bi2a–S3/Br3	× 1	129.0(5)
S1–Bi2a–S3/Br3	× 1	128.9(5)
S2/Br2–Bi2a–S3/Br3	× 1	77.3(3)
S2/Br2–Bi2a–S3/Br3	× 1	78.0(4)
S3/Br3–Bi2a–S3/Br3	× 1	81.47(13)
S1–Bi2b–S1	× 1	79.7(6)
S1–Bi2b–S1	× 1	82.4(6)
S1–Bi2b–S2/Br2	× 1	74.3(6)
S1–Bi2b–S2/Br2	× 1	73.4(5)
S1–Bi2b–S2/Br2	× 1	141.5(4)
S1–Bi2b–S2/Br2	× 1	75.4(6)
S1–Bi2b–S2/Br2	× 1	151.5(8)
S1–Bi2b–S2/Br2	× 1	74.3(6)
S1–Bi2b–S2/Br2	× 1	89.0(9)

		Bond Angle (°)
S1–Bi3–S1	× 3	99.3(9)
S1–Bi3–S1	× 3	162.40(15)
S1–Bi3–S1	× 6	69.9(2)
S1–Bi3–S1	× 3	116.6(5)
S1–Bi4–S1	× 3	101.4(8)
S1–Bi4–S1	× 2	115.2(5)
S1–Bi4–S1	× 1	115.2(6)
S1–Bi4–S1	× 3	166.10(14)
S1–Bi4–S1	× 6	70.37(15)

Table S5. Structural parameters of $Bi_{13}S_{17}Br_3$ extracted from Rietveld and PDF analyses.

		Rietveld	PDF
a (Å)		15.5069(3)	15.585(4)
c (Å)		4.01119(2)	4.0114(17)
V (Å^3)		835.318(17)	843.8(8)
x, *y*, *z*, U_{iso}	Bi1	0.61050(7), 0.48340(7), 0.9464(19) 0.0153(3)	0.6106(3), 0.4835(3), 0.941(5) 0.020(5)
	Bi2a	0.70245(10), 0.75474(8), 0.4317(19) 0.0134(3)	*Fixed at Rietveld values* 0.025(8)
	Bi2b	0.7092(6), 0.7915(5), 0.444(12) 0.0134(3)	*Fixed at Rietveld values* 0.025(8)
	Bi3	0, 0, 0.104(6) 0.0184(18)	*Fixed at Rietveld values* 0.007(1)
	Bi4	0, 0, 0.807(5) 0.0184(18)	*Fixed at Rietveld values* 0.007(1)
	Br1	2/3, 1/3, 0.428(5) 0.0238(12)	2/3, 1/3, 0.398(7) 0.032(4)
	S1	0.8341(4), 0.8137(5), 0.982(3) 0.014(2)	0.844(15), 0.826(18), 0.00(5) 0.026(5)
	S2/Br2	0.7359(3), 0.6001(4), 0.437(9) 0.0204(13)	0.735(14), 0.597(2), 0.492(10) 0.06(1)
	S3/Br3	0.5470(4), 0.6073(4), 0.924(5) 0.0068(17)	0.552(18), 0.613(19), 0.869(5) 0.032(4)
R_{wp}		5.7%	
R_w			8.5%

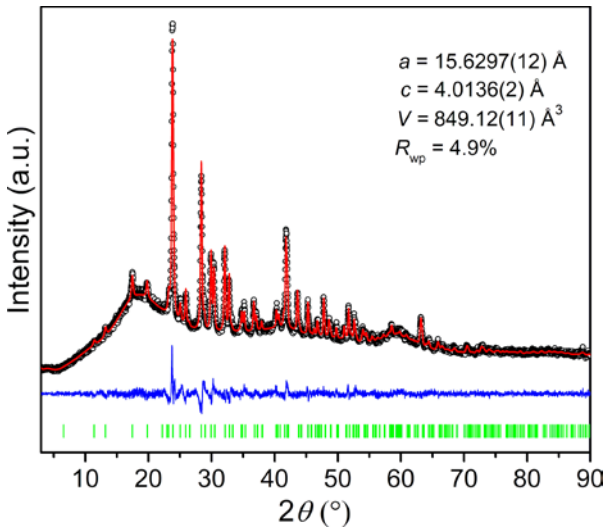

Fig. S2. Rietveld fit of lab PXRD pattern of $Bi_{13}S_{18}I_2$. Black circles, red trace, and blue trace correspond to experimental PXRD data, calculated pattern, and difference curve, respectively. Green vertical bars in the Rietveld plot indicate the calculated positions of the diffraction maxima. Extracted unit cell parameters are provided with the R_{wp} residual.

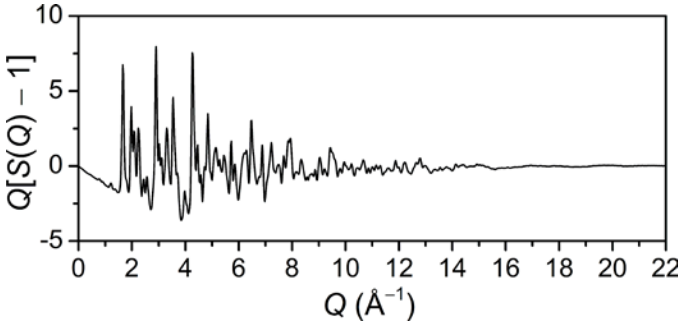

Fig. S3. Structure function of $Bi_{13}S_{17}Br_3$.

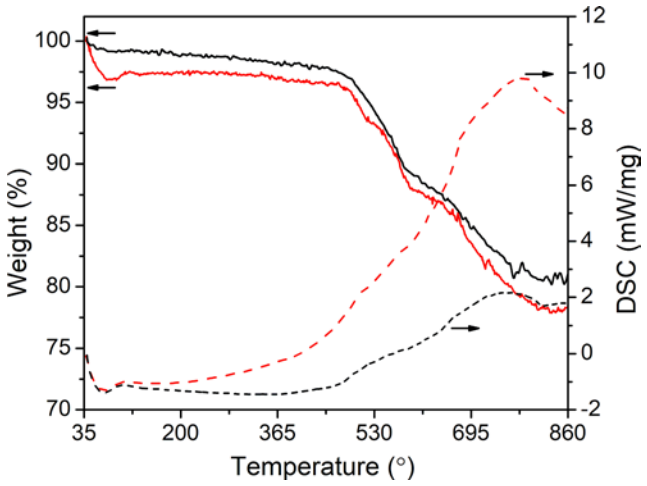

Fig. S4. TGA/DSC analysis of $Bi_{13}S_{17}Br_3$ (red trace) and $Bi_{13}S_{18}I_2$ (black trace). Solid (dashed) lines correspond to TGA (DSC) data. No thermal decomposition of the two compounds was observed up to ~450 °C.

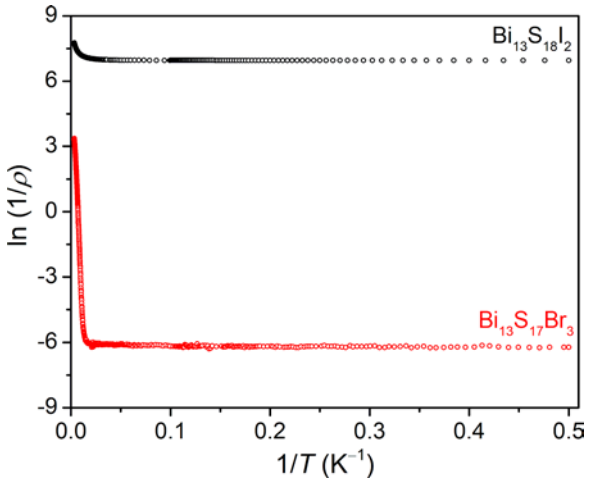

Fig. S5. The plot of $\ln(1/\rho)$ vs $(1/T)$ for $Bi_{13}S_{17}Br_3$ (red trace) and $Bi_{13}S_{18}I_2$ (black trace).